

Robust Identity Perceptual Watermark Against Deepfake Face Swapping

Tianyi Wang Mengxiao Huang Harry Cheng Bin Ma* Yinglong Wang*

Abstract

Notwithstanding offering convenience and entertainment to society, Deepfake face swapping has caused critical privacy issues with the rapid development of deep generative models. Due to imperceptible artifacts in high-quality synthetic images, passive detection models against face swapping in recent years usually suffer performance damping regarding the generalizability issue. Therefore, several studies have been attempted to proactively protect the original images against malicious manipulations by inserting invisible signals in advance. However, the existing proactive defense approaches demonstrate unsatisfactory results with respect to visual quality, detection accuracy, and source tracing ability. In this study, we propose the first robust identity perceptual watermarking framework that concurrently performs detection and source tracing against Deepfake face swapping proactively. We assign identity semantics regarding the image contents to the watermarks and devise an unpredictable and unreversible chaotic encryption system to ensure watermark confidentiality. The watermarks are encoded and recovered by jointly training an encoder-decoder framework along with adversarial image manipulations. Extensive experiments demonstrate state-of-the-art performance against Deepfake face swapping under both cross-dataset and cross-manipulation settings.

1. Introduction

The prevalent Deepfake face swapping technique has received widespread attention with the development of deep generative models. By swapping the facial identity from the source image onto the target one, Deepfake face swapping can bring convenience to people’s lives and benefit society from the perspective of human entertainment such as film-making. Nevertheless, misusing the technique has brought privacy issues to various groups of victims including celebrities, politicians, and even every human being [38]. Therefore, it is necessary to prevent malicious attacks while maintaining positive usages of Deepfake face swapping.

Most existing countermeasures [11, 19, 26, 30, 37, 41, 50] regarding Deepfake face swapping follow the pipeline of devising a deep detection model that passively investigates and analyzes the underlying synthetic artifacts to distinguish the fake images. While accomplishing progresses in the early stages, passive detection suffers the generalization challenge such that obvious performance damping occurs when detecting fake materials produced by unknown synthetic algorithms [36]. Moreover, following rapid improvements in deep generative algorithms, it has become burdensome to locate perceivable manipulation traces within high-quality synthetic images. To overcome this issue, several recent studies consider executing proactive defense against synthetic manipulations. In other words, the goal is to protect the original images by inserting imperceptible signals in advance of posting in public and being manipulated unexpectedly.

The proactive approaches can be categorized into two main strategies, namely, distorting [13, 35, 39] and watermarking [3, 25, 45]. The former learns a distortion that nullifies potential synthetic manipulations by inserting it into the original images, and the latter encodes semi-fragile watermarks into original images and determines the authenticity based on the existence of watermarks afterward. Both ways aim to proactively protect the original images without affecting the visual qualities. While demonstrating preliminary initiations, the existing approaches suffer several flaws. Firstly, in the current research stage, both the distorting and watermarking frameworks lack generalization ability on unseen datasets when facing unknown synthetic manipulations. Secondly, although the semi-fragile watermarks can help determine real and fake based on their existence, they are prone to be unstable when facing unavoidable common image processing operations. Moreover, watermarks that are fragile to malicious synthetic manipulations cannot help conduct source tracing on the victim target images simultaneously. In particular, in an integral chain of evidence for the forensic investigation in the cybercrime cases related to Deepfake face swapping, besides correctly addressing the falsification, it is crucial to retrieve intelligence information of the source materials [1, 17, 42]. In other words, tracing the original target images along with the detection task can help fulfill the evidence integrality. Lastly, while pre-

*Corresponding authors: Yinglong Wang and Bin Ma.

venting privacy issues, directly adding distortions not only unavoidably degrades the visual qualities of the images [9], but also unfavorably disables benign adoptions of Deepfake face swapping.

To address the aforementioned issues, in this study, we propose a novel robust identity perceptual watermarking framework that promotes proactive defense against Deepfake face swapping. In general, we establish and embed robust and invisible identity perceptual watermarks that are semantically meaningful into original images for detection and source tracing purposes simultaneously, while allowing benign usages of face swapping algorithms. First, based on the identities of facial images, we construct securely protected identity perceptual watermarks by introducing a chaotic encryption system. Then, we devise an end-to-end robust watermarking framework that consists of an encoder-decoder architecture to be trained with common and face swapping manipulation pools. Relying on the promising watermark recovery performance, the authenticity of a candidate image is determined by the consistency between the recovered watermark from the image and the content-matched identity perceptual watermark. The source tracing is simultaneously achieved with respect to the identity semantics carried by the recovered watermark. Extensive experiments prove the generalization ability of our proposed approach under cross-dataset and cross-manipulation settings with average watermark recovery accuracies all above 98%, strongly outperforming the contrastive methods. Our contributions can be summarized as follows:

- We propose a novel idea of identity perceptual watermarks based on image contents to proactively defend against Deepfake face swapping regarding watermark consistencies. A chaotic encryption system is collaboratively devised to ensure watermark confidentiality.
- We present an encoder-decoder framework to robustly and invisibly embed the watermarks into facial images. To the best of our knowledge, we are the first to concurrently achieve detection and source tracing for Deepfake face swapping by embedding a single watermark.
- Experiments qualitatively and quantitatively demonstrate the promising watermark recovery performance of our method along with outstanding generalization ability, outperforming the related state-of-the-art algorithms.

2. Related Work

Existing forensic investigations on Deepfake face swapping mostly rely on devising passive detectors [11, 19, 26, 30, 41, 50] that analyze traces of suspected images in various feature domains. In view of the rising challenge prompted by the improving synthetic quality, instead of searching for synthetic artifacts, proactive defense aims to protect original images by inserting imperceptible signals before potential manipulations. In other words, while malicious face swap-

ping happens after the target image is publicly posted (e.g., on Twitter or Instagram), proactive actions are performed in advance in two ways: *distortions* and *watermarks*.

2.1. Proactive Distortions

Proactive distortions [2, 14, 29, 46, 47] are usually inserted into pristine images to nullify the synthetic models following $\tilde{x} = x + \eta$, where x and \tilde{x} are the pristine images before and after the learned invisible distortion η is added, respectively. In particular, recently, Anti-Forgery [35] exploits the vulnerability of GAN-based models and super-visely learns a particular distortion in the lab color space for a specific pristine image regarding each synthetic algorithm. CMUA [13] presents a two-level perturbation fusion strategy and heuristically learns a universal distortion that can disrupt multiple synthetic algorithms. TAFIM [2] introduces image-specific perturbations with better robustness via attention-based fusion and refinement. Besides adding invisible perturbations that could heavily distort the synthetic results, Wang *et al.* [39] further promoted a detector that distinguishes the distorted images with high accuracy since it does not share similar perspectives as human eyes.

2.2. Proactive Watermarks

Digital watermarks [32] are originally used for copyright protection and authentication [7, 20, 44], and they are thus designed to have promising robustness. Ever since the occurrence of the first deep neural network (DNN) based end-to-end trainable watermarking framework, HiDDeN [51], various follow-up algorithms [6, 15, 23, 31] emerge based on the encoder-decoder architecture for robust watermarking. In specific, the encoder reconstructs a visually identical image by inserting a secret message into the original one, and the decoder takes charge of recovering the encoded message from the watermarked image. For example, Yu *et al.* [48, 49] attempted to assign particular fingerprints regarding generative models for the attribution purpose.

Different from the robust watermarking studies, FaceGuard [45] and FaceSigns [25] propose semi-fragile watermarks such that they stay robust to benign image post-processing operations but become fragile when facing malicious face manipulations. The authors claimed to distinguish fake materials if no watermark is detected in candidate images. Recently, a separable watermarking framework, SepMark [42], is conducted with two watermark decoders, a Tracer and a Detector, where the former recovers robust watermarks for source tracing, and the latter extracts semi-fragile watermarks to determine real and fake. To the best of our knowledge, robust watermarking has been barely attempted to detect Deepfake face swapping adaptively, and performing detection and source tracing simultaneously with a single watermark remains largely unexplored in the current research domain.

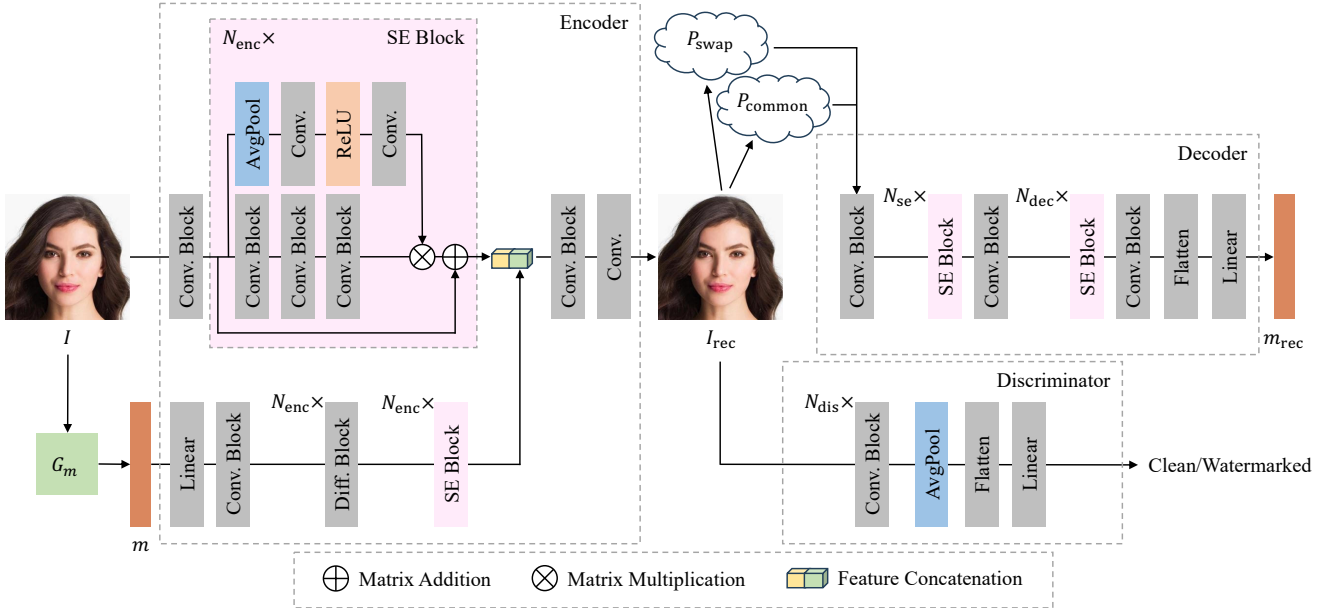


Figure 1. Framework of the proposed approach. An original clean image I is first passed to generator G_m to generate the corresponding identity perceptual watermark m . Then, I and m are fed to the encoder for watermark embedding. Manipulation pools P_{common} and P_{swap} help preserve watermark robustness during supervision. A discriminator helps maintain the visual quality. In the end, the watermark m_{rec} is recovered by passing the manipulated image to the decoder.

3. Methodology

3.1. Overview

In this paper, we propose an identity perceptual watermarking framework to adaptively embed imperceptible robust watermarks into images and proactively achieve detection and source tracing against Deepfake face swapping by precisely recovering the encoded watermarks. The model framework is demonstrated in Figure 1. First, we devise a watermark generator G_m to securely prepare the binary watermarks by assigning identity perceptual semantics with respect to the image contents. Then, the encoder is fed with the clean image I and the corresponding watermark m for encoding. To guarantee robustness, we apply common manipulation pool P_{common} and face swapping manipulation pool P_{swap} to the watermarked image I_{rec} before recovering the watermark m_{rec} via the decoder. Meanwhile, a discriminator that distinguishes the watermarked and clean images is adopted in the training stage to enhance image visual quality. By assigning constraints as discussed in Section 3.5, the framework is trained to satisfy our objectives.

In practice, for an original image I with facial identity t , the watermark m is produced by G_m and embedded into I to generate the watermarked image I_{rec} via the encoder. Upon the malicious face swapping manipulation, a synthetic facial image I_{fake} is derived by swapping identity s onto I_{rec} . By utilizing the decoder, the watermark m_{rec} which is highly consistent with m can be robustly recov-

ered from I_{fake} . Since I_{fake} contains facial identity s , its corresponding watermark m_s can be generated using G_m , and demonstrating the inconsistency between m_{rec} and m_s can accomplish the detection task on Deepfake face swapping. On the other hand, as m_{rec} is robustly recovered, the trusted original image I with watermark m can be traced by inspecting the matchings between identities and watermarks in an officially recorded hash map.

3.2. Identity Perceptual Watermarks

Unlike early frameworks that enforce random initialization, we derive the watermark for each facial image by analyzing the identity semantics. In particular, we propose an identity perceptual watermark generator G_m that generates binary watermark m with length l based on the facial identity of image I . The pipeline of G_m follows the characteristics of hashing algorithms [21, 28]: *collision free* and *one-way computational*.

Collision Free. Since the goal is to detect Deepfake face swapping by addressing inconsistencies between the recovered and content-matched watermarks of candidate images, it is necessary to ensure that no two identical watermarks belong to different facial identities. Face recognition, a task to identify different facial identities by producing distinguishable embeddings, has been proved the ability on various large datasets with reliable models. In this study, impressed by the outstanding achievements, we adopt well-performed face recognition algorithms that retrieve identity

embeddings in the form of high-dimensional vectors. To match up the required watermark length l , we first select a large dataset that contains sufficient unique identities and retrieve the identity embeddings E with dimension d_E accordingly. Then, we apply the principal component analysis (PCA) [27] to E and learn a transform rule ϕ that projects the identity embeddings of the images from dimension d_E down to l while optimally preserving the original correlations between facial identities with respect to the principal components. Thereafter, for the purpose of constructing binary watermarks, we conduct a unit-variance scaling on the projected embeddings E_{pca} to the range between 0 and 1 by

$$E_{\text{scale}} = \frac{E_{\text{pca}} - \min(E_{\text{pca}})}{\max(E_{\text{pca}}) - \min(E_{\text{pca}})}, \quad (1)$$

where E_{scale} denotes the scaled embeddings with respect to the standard deviation, which favorably preserves the distribution of E_{pca} . In the end, we set a cutoff value $0 \leq c \leq 1$ to round the entries of E_{scale} to binary values accordingly and obtain the identity perceptual watermarks E_{binary} . Besides, a watermark collision check is arranged in Section 4.4 to validate the collision-free characteristic.

One-Way Computational. Since we concurrently conduct detection and source tracing, an adversary with sufficient knowledge of our work may aim to replace the encoded watermark with a content-matched one. To prevent hostile attacks [5, 33], we enforce the watermark to be one-way computational, that is, it is insufficient to recover the watermark construction pipeline by merely acquiring the watermark from the image. Specifically, besides keeping ϕ encapsulated, we apply chaotic encryption [24] on E_{binary} using a logistic map

$$x_{i+1} = rx_i(1 - x_i), \quad (2)$$

where constants x_0 at $i = 0$ and r are the initial condition and control parameter, respectively. x_i denotes the i -th value in the chaotic map and $0 \leq i < l$. The values in $X = \{x_1, x_2, \dots, x_l\}$ are derived accordingly, and a binary encryption key $K = \{k_1, k_2, \dots, k_l\}$ is computed via

$$k_i = \lfloor x_i p^q \bmod 2 \rfloor, \quad (3)$$

where p and q are pre-defined prime constants. Finally, the encrypted identity perceptual watermark m for image I is derived by a logical exclusive OR (XOR) operation between K and the unencrypted watermark from E_{binary} . Relying on the sensitive dependence on the initial condition and chaotic map nonlinearity characteristics, the final watermarks leveraged in the watermarking framework are unpredictable and nonreversible unless having access to Eqn.(2) and Eqn.(3) including the critical constant coefficients. Specifically, the entry values in X vary drastically with respect to the values of x_0 and r , and the watermarks are thus securely protected.

On the contrary, with authority on K , performing an extra XOR operation on m using K can easily decrypt the watermarks back to the ones in E_{scale} to trace back for the identity information.

3.3. Watermark Encoding

For an input image I , we encode the watermark m using an encoder that is mainly based on convolutional neural networks (CNN) with squeeze-and-excitation networks (SENet) [10] and diffusion blocks. Specifically, the image features and watermark features are separately analyzed and then concatenated to reconstruct the watermarked image I_{rec} .

Image Features. In this paper, we preserve the width and height of I in the propagation process to avoid information loss in image reconstruction. We first feed I to a convolutional block (denoted as Conv. Block) that contains a CNN layer, a batch normalization layer, and a ReLU activation function in a sequential order to exaggerate the number of feature channels. Squeeze-and-excitation network (SENet) [10], an on-the-shelf mechanism that improves channel interdependencies, can favorably perform feature recalibration on the input image. As depicted in Figure 1, N_{enc} repeated SENets (denoted as SE Block) are applied to seek proper channels and elements within the feature map for watermark encoding without jeopardizing the visual quality.

Watermark Features. As for the binary identity perceptual watermark m of length l , we first increase the length linearly via a fully connected layer followed by dimension expansion via shape rearrangement and then leverage a convolutional block to elaborate the channel perspective. After that, we devise N_{enc} consecutive diffusion blocks (denoted as Diff. Block) utilizing deconvolutions and smoothly diffuse the feature elements that represent m to the same dimension as the width and height of I . Similarly, a series of N_{enc} SE Blocks is promoted for the preparation of watermarking.

Image Reconstruction. Lastly, features of I and m are concatenated with respect to the channel dimension followed by a convolutional block and a vanilla CNN layer to reconstruct the image I_{rec} that is visually identical to I .

3.4. Watermark Recovery

Manipulation Pools. In real-life scenarios, images inevitably suffer degradation by common post-processing operations and noises such as compression and blurring upon uploading and spreading on social media. Therefore, to satisfy the objectives, as shown in Figure 1, we construct two manipulation pools, P_{common} and P_{swap} , to supervise the proposed framework. On the one hand, the common manipulation pool P_{common} includes the benign post-processing operations that are commonly seen in the real world. On the

other hand, we enclose Deepfake face swapping models in the face swapping pool P_{swap} to preserve robustness when facing malicious attacks.

Decoder. We fed the post-manipulation image to the decoder for watermark recovery. The decoder follows a reverse pipeline of the encoder. In particular, after extracting features back to a large number of channels, we apply N_{se} SE Blocks, where $N_{\text{se}} = N_{\text{dec}} + 3$, to gradually expand the number of channels and seek the determinant elements that hide the watermark information. Then, N_{dec} SE Blocks without channel modification are performed after narrowing down the number of channels. In the end, a convolutional block, a flattening operation, and a linear projection are sequentially applied to recover the watermark m_{rec} .

3.5. Objective Functions

During the training stage, we employ a total of 4 loss functions for guidance, namely, *reconstruction loss*, *recovery loss*, *adversarial loss*, and *generative loss*.

Reconstruction Loss. We embed the watermarks into images and pursue the uttermost similarity between the original and watermarked images by assigning a pixel-wise L_2 constraint on the encoder,

$$L_{\text{enc}} = \|\text{Enc}(\theta_{\text{enc}}, I, m) - I\|_2, \quad (4)$$

where I denotes the clean image before watermarking, m represents the watermark, and θ_{enc} encloses the parameters of the encoder $\text{Enc}(\cdot)$.

Recovery Loss. Similarly, a bit-wise L_2 constraint is applied on the decoder for watermark recovery,

$$L_{\text{dec}} = \|\text{Dec}(\theta_{\text{dec}}, \text{Enc}(\theta_{\text{enc}}, I, m)) - m\|_2, \quad (5)$$

where θ_{dec} refers to the parameters of the decoder $\text{Dec}(\cdot)$. At the same time, the encoder is updated alongside.

Adversarial Loss. Following the convention of robust watermarking [15, 23, 51], a discriminator D with parameters θ_d is applied to improve visual qualities of the images following

$$L_{\text{adv}} = -\mathbb{E}(\log(D(\theta_d, I))) + \mathbb{E}(\log(1 - D(\theta_d, \text{Enc}(\theta_{\text{enc}}, I, m)))) \cdot N_{\text{dis}} \quad (6)$$

The discriminator is implemented as a binary classifier with N_{dis} convolutional blocks, and it adversarially learns to identify clean and watermarked images on each pair of I and I_{rec} during model supervision.

Generative Loss. When training with the face swapping manipulation pool P_{swap} , we arrange an extra objective using an L_2 constraint to make sure the embedded watermarks do not affect the synthetic results following

$$L_{\text{gen}} = \|G(I, I_s) - G(\text{Enc}(\theta_{\text{enc}}, I, m), I_s)\|_2, \quad (7)$$

where I_s is the image that provides identity information for the face swapping model $G(\cdot)$.

Overall Objective Function. Coefficients λ_{enc} , λ_{dec} , λ_{adv} , and λ_{gen} are assigned to compute the weighted sum in the overall objectives L_{common} and L_{swap} for P_{common} and P_{swap} following

$$L_{\text{common}} = \lambda_{\text{enc}}L_{\text{enc}} + \lambda_{\text{dec}}L_{\text{dec}} + \lambda_{\text{adv}}L_{\text{adv}}, \quad (8)$$

and

$$L_{\text{swap}} = L_{\text{common}} + \lambda_{\text{gen}}L_{\text{gen}}. \quad (9)$$

4. Experiment

4.1. Implementation Details

Datasets. Experiments are conducted on the high-quality CelebA-HQ dataset [16] with 6,217 unique identities following the official split [22] for training, validation, and testing. To further validate the generalization ability, we tested the trained model on the Labeled Faces in the Wild (LFW) dataset [12] with 5,749 unique identities.

Manipulation Pools. P_{common} consists of the following manipulations for both training and testing: Dropout, Resize, Jpeg Compression, Gaussian Noise, Salt and Pepper, Gaussian Blur, and Median Blur. P_{swap} includes SimSwap [4] solely in the training phase and adopts SimSwap, InfoSwap [8], and UniFace [43] with state-of-the-art performance for cross-manipulation evaluation in the testing phase. Since there are various common manipulations to be considered and they only bring noises without modifying the facial contents, we first pre-trained the model using P_{common} for sufficient iterations. Thenceforth, we slowly fine-tuned it with the help of P_{swap} by introducing random images that provide different facial identities for swapping onto I_{rec} .

Parameters. Upon watermark generation, CelebA-HQ is adopted to derive the transform rule ϕ with cutoff value $c = 0.5$, and we set $x_0 = 0.1$, $r = 3.93$, $p = 5$, and $q = 11$ for the constant coefficients in Eqn.(2) and Eqn.(3). We conducted watermark encoding with lengths 64 and 128 for images at 128×128 and 256×256 resolutions, respectively, and we set N_{enc} to 3 and 4, N_{dec} to 1 and 2, and N_{dis} to 3 and 4 for the two resolutions. In this study, we trained the proposed model in two steps. The proposed approach is firstly trained with P_{common} by setting $\lambda_{\text{enc}} = 1$, $\lambda_{\text{dec}} = 10$, and $\lambda_{\text{adv}} = 0.01$ with a learning rate of $1e - 3$ to guarantee the promising watermark recovery performance regarding common manipulations. Then, the trained model is further tuned on SimSwap by setting $\lambda_{\text{enc}} = 10$, $\lambda_{\text{dec}} = 1$, $\lambda_{\text{adv}} = 0.01$, and $\lambda_{\text{gen}} = 5$ with a lower learning rate of $1e - 5$. This process mildly adjusts the framework to stay robust when facing both common and face swapping manipulations. Adam optimizers [18] are adopted through the entire training pipeline for each model component. Our model is implemented using PyTorch on 4 Tesla A100 GPUs with a batch size of 32.



Figure 2. Visual effects of common and face swapping manipulations on the watermarked images. The raw and watermarked images are displayed in the first two rows, respectively. Manipulated outputs via different operations on the watermarked images are placed in row 3. Face swapping results on the watermarked target images are exhibited in the last three columns while the source images that provide identity information are omitted.

Model	Resolution	Length	PSNR \uparrow	SSIM \uparrow
HiDDeN [51]	128 \times 128	30	33.26	0.888
MBRS [15]	128 \times 128	30	33.01	0.775
CIN [23]	128 \times 128	30	43.37	0.967
RootAttr [48]	128 \times 128	100	43.93	0.975
Ours	128 \times 128	64	47.39	0.993
AntiForgery [35]	256 \times 256	–	35.62	0.953
CMUA [13]	256 \times 256	–	38.64	0.857
MBRS [15]	256 \times 256	256	44.14	0.969
FaceSigns [25]	256 \times 256	128	36.99	0.889
Ours	256 \times 256	128	45.38	0.994

Table 1. Quantitative visual quality evaluation of the watermarked images. Information includes model name, image resolution, watermark length, PSNR, and SSIM.

4.2. Experiment on CelebA-HQ

In this section, experiments are conducted on the testing set of CelebA-HQ. Since no existing work has performed detection and source tracing on face swapping images using a single watermark to our knowledge, we selected the robust watermarking frameworks (HiDDeN [51], MBRS [15], CIN [23], and RootAttr [48]), proactive semi-fragile Deepfake watermarking frameworks (FaceSigns [25]), and proactive Deepfake distortion frameworks (AntiForgery [35] and CMUA [13]) for comparison. For fairness, the publicly available trained model weights that correspond to optimal performance are directly adopted.

4.2.1 Qualitative Evaluation

We visualized randomly drafted images to validate the visual quality of the watermarked images. As exhibited in Figure 2, despite knowing the existence of the watermarks, differences between the raw and watermarked images in the first and second rows, respectively, are visually imperceptible. In row 3, we illustrated the visual effects of the common and face swapping manipulations. For simplicity, faces that provide identity information for face swapping in the last three columns are omitted in the exhibition. It is worth noting that no distortion can be observed in the face swapping results in the last three columns. In other words, the encoded watermarks do not affect the visual qualities of the synthetic faces.

4.2.2 Quantitative Evaluation

Visual Quality. We employed the average peak signal-to-noise ratio (PSNR) and structural similarity index measure (SSIM) [40] between the raw and watermarked images to evaluate the visual quality of watermarked images. As Table 1 reports, while the goal of embedding watermarks into raw images imperceptibly stands for all contrastive methods, our proposed approach achieves the state-of-the-art visual quality in terms of PSNR and SSIM at both resolution levels. Meanwhile, it can be observed that although pursuing the same objective in visual quality, the proactive distortion models, AntiForgery and CMUA, have revealed relatively unsatisfactory performance since the noises and perturbations are directly added to raw images while image reconstructions are executed in watermarking.

Watermark Recovery on Common Manipulations. The watermarks are represented via binary values, and the bit-

Manipulations	HiDDeN	MBRS	CIN	RootAttr	Ours	MBRS	FaceSigns	Ours
	[51] 128 × 128	[15] 128 × 128	[23] 128 × 128	[48] 128 × 128	128 × 128	[15] 256 × 256	[25] 256 × 256	256 × 256
Dropout	82.44%	100.00%	100.00%	94.76%	99.99%	99.19%	55.36%	99.99%
Resize	82.01%	100.00%	99.17%	99.94%	100.00%	100.00%	98.63%	99.08%
Jpeg	67.84%	99.49%	96.86%	66.85%	99.48%	99.69%	82.64%	99.99%
GaussianNoise	51.36%	99.60%	86.00%	60.18%	98.63%	58.31%	53.61%	99.97%
SaltPepper	52.30%	99.37%	93.95%	66.62%	95.54%	65.33%	73.95%	97.54%
GaussianBlur	73.04%	100.00%	100.00%	99.95%	100.00%	72.05%	98.68%	97.93%
MedBlur	82.72%	100.00%	97.03%	99.98%	100.00%	98.06%	99.86%	99.01%
Average	70.24%	99.78%	96.14%	84.04%	99.09%	84.66%	80.39%	99.07%
SimSwap [4]	50.02%	49.98%	50.28%	50.00%	99.99%	50.00%	49.74%	99.98%
InfoSwap [8]	50.07%	50.82%	50.60%	50.01%	99.31%	50.71%	50.00%	99.73%
UniFace [43]	54.98%	50.22%	46.01%	71.15%	99.57%	49.98%	50.59%	94.86%
Average	51.69%	50.34%	48.96%	57.05%	99.62%	50.23%	50.11%	98.19%

Table 2. Quantitative comparison on CelebA-HQ regarding the bit-wise watermark accuracy of the watermarks under common manipulations and malicious face swapping manipulations.

wise accuracy of the recovered watermark is computed by comparing it to the original watermark following

$$\text{ACC}(m_{\text{rec}}, m) = \frac{l - d_{\text{ham}}(m_{\text{rec}}, m)}{l}, \quad (10)$$

where d_{ham} computes the hamming distance [34] between the recovered and original watermarks m_{rec} and m , and l refers to the watermark length. In the experiment, each type of manipulation in P_{common} and P_{swap} is performed before extracting the watermarks. Watermark recovery performance in the comparative experiment is reported in Table 2. Specifically, considering the common manipulations, our method outperforms HiDDeN, CIN, and RootAttr at 128×128 resolutions with a better average accuracy, and our performance is competitive against MBRS with an acceptable average accuracy above 99%. However, it can be observed from Table 1 that MBRS heavily suffers visual quality issues with unsatisfactory PSNR and SSIM values (33.01 and 0.775) in order to achieve the best bit-wise watermark recovery accuracy in Table 2. As for the 256×256 resolution, we reached an average accuracy of 99.07% on the common manipulations, outperforming the existing state-of-the-art methods. On the contrary, although accomplishes reasonable visual quality in Table 1, MBRS experiences a large performance damping on the common manipulations with respect to the watermark recovery accuracy compared to the 128×128 resolution version.

Watermark Recovery on Face Swapping. In this paper, the face swapping manipulation pool contains merely SimSwap [4] in the training phase, and we validated the watermark recovery performance for both in- and cross-manipulation settings by introducing other recent state-of-the-art face swapping algorithms, InfoSwap [8] and Uni-

Face [43], in the testing phase. As a result, our model consistently recovers the desired watermark messages at average accuracies of 99.62% and 98.19% for 128×128 and 256×256 resolutions, respectively, while CIN and MBRS both obtain accuracies around 50% and RootAttr has accuracies below 75% against all synthetic models. Moreover, it can be concluded from the cross-manipulation tests on unseen synthetic models that by simply tuning with SimSwap, the hidden watermarks are pleasantly maintained by our method since the goals for face swapping are identical. Meanwhile, the semi-fragile watermarking framework, FaceSigns, although obtains low recovery accuracies as designed when facing synthetic manipulations that are expected to destroy the embedded watermarks, its performance regarding the common ones is unexpectedly unsatisfactory besides illustrating low visual quality as reported in Table 1, leading to an average recovery accuracy of 80.39%.

Discussion. In general, Salt and Pepper and Gaussian Noise are the most challenging common manipulations that cause fluctuations in the watermark recovery accuracies for all watermarking methods as summarized in Table 2. This is consistent with the visualization results in Figure 2 (col. 4 & 7) such that these manipulations add a plethora of perceivable noises to the images and thus heavily jeopardize the hidden watermarks. On the other hand, the robust watermarking frameworks fail to maintain robustness when facing the state-of-the-art face swapping models. As a result, our proposed model is the only one that maintains the bit-wise watermark recovery accuracies above 95% for all common manipulations and above 90% for all face swapping manipulations, while other methods are heavily affected by at least one of the manipulations.

4.3. Cross-Dataset Experiment

We further evaluated our watermarking framework on an unseen dataset, Labeled Faces in the Wild (LFW) [12], regarding the generalization ability. Since images in LFW are at 250×250 resolutions, we only conducted experiments using the 256×256 resolution watermarking frameworks by slightly upsampling the image sizes. Performance evaluations with respect to visual quality and watermark recovery accuracy are listed in Table 3 and Table 4, respectively. Similar results can be summarized even on a different dataset. In particular, MBRS [15] and our approach execute watermarking with promising visual qualities while FaceSigns [25] fails to do so. Meanwhile, the challenging manipulations concluded in Section 4.2 consistently lead to unsatisfactory bit-wise watermark recovery accuracies in this section. As a result, although slightly affected by Salt and Pepper (95.99%) and Gaussian Blur (97.11%), we successfully maintained state-of-the-art accuracies above 95% for all manipulations. Furthermore, an obvious accuracy decline on UniFace [43] can be observed in Table 2 and Table 4 at 256×256 resolutions on both CelebA-HQ [16] and LFW. Besides the challenges caused by cross manipulation, this is mainly due to the setting of accepting only half precision floating-points inputs by UniFace. Although the synthetic pipeline is unaffected, this can lead to discrepancies in the watermark recovery process because of information loss.

4.4. Watermark Collision Check

As introduced in Section 3.2, the binary identity perceptual watermarks are derived from identity embeddings generated via well-designed face recognition tools¹. To validate the claim that the watermarks retain the collision-free characteristic of the original identity embeddings, we performed collision checks at different watermark lengths. In specific, for the sets of watermarks M_i and M_j of a pair of arbitrary identities i and j , the following statement stands,

$$\forall x \in M_i \forall y \in M_j (x \neq y). \quad (11)$$

In other words, identical watermarks are not allowed to be derived from images that belong to different identities.

In this paper, images from CelebA-HQ with 6,217 unique identities are adopted to establish ϕ for watermarking, and watermarks of images in LFW with 5,749 unseen identities are derived following the rule accordingly. As a result, there is no collision in the experiment for CelebA-HQ and LFW at both 128×128 and 256×256 resolutions. Meanwhile, upon passing the collision check even though not seeing the identities in LFW when defining ϕ , it can be concluded that the number of unique identities in CelebA-

¹<https://github.com/serengil/deepface>

Metrics	MBRS [15]	FaceSigns [25]	Ours
PSNR \uparrow	45.37	38.23	45.42
SSIM \uparrow	0.969	0.910	0.994

Table 3. Quantitative visual quality evaluation of the watermarked images on LFW.

Manipulations	MBRS [15]	FaceSigns [25]	Ours
Dropout	99.30%	56.45%	99.97%
Resize	100.00%	98.91%	98.16%
Jpeg	99.08%	75.64%	99.99%
GaussianNoise	55.61%	59.90%	99.92%
SaltPepper	61.15%	67.99%	95.99%
GaussianBlur	73.93%	99.01%	97.11%
MedBlur	99.38%	99.91%	98.13%
Average	84.06%	79.69%	98.47%
SimSwap [4]	50.04%	49.77%	99.96%
InfoSwap [8]	50.23%	49.91%	98.67%
UniFace [43]	50.18%	52.25%	97.06%
Average	50.15%	50.64%	98.56%

Table 4. Quantitative comparison on LFW regarding the bit-wise watermark accuracy of the watermarks under common manipulations and malicious face swapping manipulations.

HQ is sufficient to avoid the potential bias, and the cross-dataset performance is therefore preserved.

5. Conclusion

In this paper, we propose a robust identity perceptual watermarking framework that proactively defends against malicious Deepfake face swapping. By securely assigning identity semantics to the watermarks, our approach concurrently accomplishes detection and source tracing with a single robust watermark for the first time. Meanwhile, the confidentiality is guaranteed by devising an unpredictable chaotic encryption system on the identity perceptual watermarks. Extensive experimental results have proved that our method is robust when facing both common and malicious manipulations on the watermarked images even under cross-dataset settings. Moreover, by leveraging a single Deepfake face swapping algorithm for fine-tuning, we are able to preserve promising cross-manipulation performance against unseen face swapping algorithms. Admittedly, since the watermarks are identity perceptual, the proposed framework is unable to detect face re-enactment manipulations that retain facial identities. Our future work will focus on designing a unified framework to proactively defend against both face swapping and face re-enactment manipulations by analyzing and introducing facial attribute features.

References

- [1] Turker Akyuz and Ibrahim Sogukpinar. Packet marking with distance based probabilities for ip traceback. In *2009 First International Conference on Networks & Communications*, pages 433–438, 2009. 1
- [2] Shivangi Aneja, Lev Markhasin, and Matthias Nießner. Tafim: Targeted adversarial attacks against facial image manipulations. In *ECCV*, pages 58–75, 2022. 2
- [3] Nicolas Beuve, Wassim Hamidouche, and Olivier Déforges. Waterloo: Protect images from deepfakes using localized semi-fragile watermark. In *Proceedings of the IEEE/CVF International Conference on Computer Vision (ICCV) Workshops*, pages 393–402, 2023. 1
- [4] Renwang Chen, Xuanhong Chen, Bingbing Ni, and Yanhao Ge. Simswap: An efficient framework for high fidelity face swapping. In *ACM MM*, page 2003–2011, New York, NY, USA, 2020. Association for Computing Machinery. 5, 7, 8
- [5] I. J. Cox, M. L. Miller, and J. A. Bloom. *Digital Watermarking*. Morgan Kaufmann Publishers, San Francisco, 2002. 4
- [6] Han Fang, Zhaoyang Jia, Zehua Ma, Ee-Chien Chang, and Weiming Zhang. Pimog: An effective screen-shooting noise-layer simulation for deep-learning-based watermarking network. In *ACM MM*, page 2267–2275, 2022. 2
- [7] Guanhao Gan, Yiming Li, Dongxian Wu, and Shu-Tao Xia. Towards robust model watermark via reducing parametric vulnerability. *ICCV*, 2023. 2
- [8] Gege Gao, Huaibo Huang, Chaoyou Fu, Zhaoyang Li, and Ran He. Information bottleneck disentanglement for identity swapping. In *CVPR*, pages 3403–3412, 2021. 5, 7, 8
- [9] Ziwen He, Wei Wang, Weinan Guan, Jing Dong, and Tieniu Tan. Defeating deepfakes via adversarial visual reconstruction. In *ACM MM*, page 2464–2472. Association for Computing Machinery, 2022. 2
- [10] Jie Hu, Li Shen, and Gang Sun. Squeeze-and-excitation networks. In *CVPR*, pages 7132–7141, 2018. 4
- [11] B. Huang, Z. Wang, J. Yang, J. Ai, Q. Zou, Q. Wang, and D. Ye. Implicit identity driven deepfake face swapping detection. In *CVPR*, pages 4490–4499, 2023. 1, 2
- [12] Gary B. Huang, Marwan Mattar, Honglak Lee, and Erik Learned-Miller. Learning to align from scratch. In *NeurIPS*, 2012. 5, 8
- [13] Hao Huang, Yongtao Wang, Zhaoyu Chen, Yuze Zhang, Yuheng Li, Zhi Tang, Wei Chu, Jingdong Chen, Weisi Lin, and Kai-Kuang Ma. Cmua-watermark: A cross-model universal adversarial watermark for combating deepfakes. *AAAI*, 36(1):989–997, 2022. 1, 2, 6
- [14] Qidong Huang, Jie Zhang, Wenbo Zhou, Weiming Zhang, and Nenghai Yu. Initiative defense against facial manipulation. *AAAI*, 35(2):1619–1627, 2021. 2
- [15] Zhaoyang Jia, Han Fang, and Weiming Zhang. Mbrs: Enhancing robustness of dnn-based watermarking by mini-batch of real and simulated jpeg compression. In *ACM MM*, 2021. 2, 5, 6, 7, 8
- [16] Tero Karras, Timo Aila, Samuli Laine, and Jaakko Lehtinen. Progressive growing of GANs for improved quality, stability, and variation. In *ICLR*, 2018. 5, 8
- [17] Hyungseok Kim, Eunjin Kim, Seungmo Kang, and Huy Kang Kim. Network forensic evidence generation and verification scheme (nfevgs). *Telecommunication Systems*, 60:261–273, 2015. 1
- [18] Diederik P. Kingma and Jimmy Ba. Adam: A method for stochastic optimization. In *ICLR*, 2015. 5
- [19] Lingzhi Li, Jianmin Bao, Ting Zhang, Hao Yang, Dong Chen, Fang Wen, and Baining Guo. Face x-ray for more general face forgery detection. In *CVPR*, pages 5000–5009, 2020. 1, 2
- [20] Li Li, Yu Bai, Ching-Chun Chang, Yunyuan Fan, Wei Gu, and Mahmoud Emam. Anti-pruning multi-watermarking for ownership proof of steganographic autoencoders. *Journal of Information Security and Applications*, 76:103548, 2023. 2
- [21] Yuenan Li, Dongdong Wang, and Linlin Tang. Robust and secure image fingerprinting learned by neural network. *IEEE TCSVT*, 30(2):362–375, 2020. 3
- [22] Ziwei Liu, Ping Luo, Xiaogang Wang, and Xiaoou Tang. Deep learning face attributes in the wild. In *ICCV*, 2015. 5
- [23] Rui Ma, Mengxi Guo, Yi Hou, Fan Yang, Yuan Li, Huizhu Jia, and Xiaodong Xie. Towards blind watermarking: Combining invertible and non-invertible mechanisms. In *ACM MM*, pages 1532–1542, 2022. 2, 5, 6, 7
- [24] Robert Matthews. On the derivation of a “chaotic” encryption algorithm. *Cryptologia*, 13(1):29–42, 1989. 4
- [25] Paarth Neekhara, Shehzeen Hussain, Xinqiao Zhang, Ke Huang, Julian McAuley, and Farinaz Koushanfar. Facesigns: Semi-fragile neural watermarks for media authentication and countering deepfakes, 2022. 1, 2, 6, 7, 8
- [26] Utkarsh Ojha, Yuheng Li, and Yong Jae Lee. Towards universal fake image detectors that generalize across generative models. In *CVPR*, 2023. 1, 2
- [27] Karl Pearson. On lines and planes of closest fit to systems of points in space, 1901. 4
- [28] Chuan Qin, Enli Liu, Guorui Feng, and Xinpeng Zhang. Perceptual image hashing for content authentication based on convolutional neural network with multiple constraints. *IEEE TCSVT*, 31(11):4523–4537, 2021. 3
- [29] Nataniel Ruiz, Sarah Adel Bargal, and Stan Sclaroff. Disrupting deepfakes: Adversarial attacks against conditional image translation networks and facial manipulation systems. In *ECCVW*, pages 236–251, 2020. 2
- [30] Andreas Rössler, Davide Cozzolino, Luisa Verdoliva, Christian Riess, Justus Thies, and Matthias Niessner. Faceforensics++: Learning to detect manipulated facial images. In *ICCV*, pages 1–11, 2019. 1, 2
- [31] Matthew Tancik, Ben Mildenhall, and Ren Ng. Stegastamp: Invisible hyperlinks in physical photographs. In *CVPR*, pages 2114–2123, 2020. 2
- [32] Andrew Tirkel, G.A. Rankin, Ron van Schyndel, W. Ho, N. Mee, and C. Osborne. Electronic watermark. In *Digital Image Computing, Technology and Applications*, 1994. 2
- [33] Sonam Tyagi, Harsh Vikram Singh, Raghav Agarwal, and Sandeep Kumar Gangwar. Digital watermarking techniques for security applications. In *2016 International Conference on Emerging Trends in Electrical Electronics & Sustainable Energy Systems (ICETEESSES)*, pages 379–382, 2016. 4

- [34] William M. Waggener. *Pulse Code Modulation Techniques*. Springer, 1995. 7
- [35] Run Wang, Ziheng Huang, Zhikai Chen, Li Liu, Jing Chen, and Lina Wang. Anti-forgery: Towards a stealthy and robust deepfake disruption attack via adversarial perceptual-aware perturbations. In *IJCAI*, pages 761–767, 2022. 1, 2, 6
- [36] Sheng-Yu Wang, Oliver Wang, Richard Zhang, Andrew Owens, and Alexei A Efros. Cnn-generated images are surprisingly easy to spot...for now. In *CVPR*, 2020. 1
- [37] Tianyi Wang and Kam Pui Chow. Noise based deepfake detection via multi-head relative-interaction. *AAAI*, 37(12): 14548–14556, 2023. 1
- [38] Tianyi Wang, Xin Liao, Kam Pui Chow, Xiaodong Lin, and Yinglong Wang. Deepfake detection: A comprehensive study from the reliability perspective, 2023. 1
- [39] Xueyu Wang, Jiajun Huang, Siqi Ma, Surya Nepal, and Chang Xu. Deepfake disrupter: The detector of deepfake is my friend. In *CVPR*, pages 14920–14929, 2022. 1, 2
- [40] Zhou Wang, A.C. Bovik, H.R. Sheikh, and E.P. Simoncelli. Image quality assessment: from error visibility to structural similarity. *IEEE TIP*, 13(4):600–612, 2004. 6
- [41] Z. Wang, J. Bao, W. Zhou, W. Wang, and H. Li. Altfreezing for more general video face forgery detection. In *CVPR*, pages 4129–4138, 2023. 1, 2
- [42] Xiaoshuai Wu, Xin Liao, and Bo Ou. Sepmark: Deep separable watermarking for unified source tracing and deepfake detection. In *ACM MM*, 2023. 1, 2
- [43] Chao Xu, Jiangning Zhang, Yue Han, Guanzhong Tian, Xi-anfang Zeng, Ying Tai, Yabiao Wang, Chengjie Wang, and Yong Liu. Designing one unified framework for high-fidelity face reenactment and swapping. In *ECCV*, pages 54–71, 2022. 5, 7, 8
- [44] P. Yang, Y. Lao, and P. Li. Robust watermarking for deep neural networks via bi-level optimization. In *ICCV*, pages 14821–14830, 2021. 2
- [45] Yuankun Yang, Chenyue Liang, Hongyu He, Xiaoyu Cao, and Neil Zhenqiang Gong. Faceguard: Proactive deepfake detection, 2021. 1, 2
- [46] Chin-Yuan Yeh, Hsi-Wen Chen, Shang-Lun Tsai, and Shang-De Wang. Disrupting image-translation-based deepfake algorithms with adversarial attacks. In *2020 IEEE Winter Applications of Computer Vision Workshops (WACVW)*, pages 53–62, 2020. 2
- [47] Chin-Yuan Yeh, Hsi-Wen Chen, Hong-Han Shuai, De-Nian Yang, and Ming-Syan Chen. Attack as the best defense: Nullifying image-to-image translation gans via limit-aware adversarial attack. In *ICCV*, pages 16168–16177, 2021. 2
- [48] Ning Yu, Vladislav Skripniuk, Sahar Abdelnabi, and Mario Fritz. Artificial fingerprinting for generative models: Rooting deepfake attribution in training data. In *ICCV*, pages 14448–14457, 2021. 2, 6, 7
- [49] Ning Yu, Vladislav Skripniuk, Dingfan Chen, Larry Davis, and Mario Fritz. Responsible disclosure of generative models using scalable fingerprinting. In *ICLR*, 2022. 2
- [50] Hanqing Zhao, Tianyi Wei, Wenbo Zhou, Weiming Zhang, Dongdong Chen, and Nenghai Yu. Multi-attentional deepfake detection. In *CVPR*, pages 2185–2194, 2021. 1, 2
- [51] Jiren Zhu, Russell Kaplan, Justin Johnson, and Li Fei-Fei. Hidden: Hiding data with deep networks. In *ECCV*, pages 682–697, 2018. 2, 5, 6, 7